AMERICAN SOCIETY FOR MICROBIOLOGY | Applied and Environmental Microbiology

Antimicrobial Effects of Free Nitrous Acid on *Desulfovibrio vulgaris*: Implications for Sulfide-Induced Corrosion of Concrete

Shu-Hong Gao,[a] Jun Yuan Ho,[a] Lu Fan,[a,b] David J. Richardson,[c] Zhiguo Yuan,[a] Philip L. Bond[a]

Advanced Water Management Centre, The University of Queensland, St. Lucia, Brisbane, Queensland, Australia[a]; iCarbonX, Shenzhen, China[b]; School of Biological Sciences, University of East Anglia, Norwich Research Park, Norwich, United Kingdom[c]

ABSTRACT

Hydrogen sulfide produced by sulfate-reducing bacteria (SRB) in sewers causes odor problems and asset deterioration due to the sulfide-induced concrete corrosion. Free nitrous acid (FNA) was recently demonstrated as a promising antimicrobial agent to alleviate hydrogen sulfide production in sewers. However, details of the antimicrobial mechanisms of FNA are largely unknown. Here, we report the multiple-targeted antimicrobial effects of FNA on the SRB *Desulfovibrio vulgaris* Hildenborough by determining the growth, physiological, and gene expression responses to FNA exposure. The activities of growth, respiration, and ATP generation were inhibited when exposed to FNA. These changes were reflected in the transcript levels detected during exposure. The removal of FNA was evident by nitrite reduction that likely involved nitrite reductase and the poorly characterized hybrid cluster protein, and the genes coding for these proteins were highly expressed. During FNA exposure, lowered ribosome activity and protein production were detected. Additionally, conditions within the cells were more oxidizing, and there was evidence of oxidative stress. Based on an interpretation of the measured responses, we present a model depicting the antimicrobial effects of FNA on *D. vulgaris*. These findings provide new insight for understanding the responses of *D. vulgaris* to FNA and will provide a foundation for optimal application of this antimicrobial agent for improved control of sewer corrosion and odor management.

IMPORTANCE

Hydrogen sulfide produced by SRB in sewers causes odor problems and results in serious deterioration of sewer assets that requires very costly and demanding rehabilitation. Currently, there is successful application of the antimicrobial agent free nitrous acid (FNA), the protonated form of nitrite, for the control of sulfide levels in sewers (G. Jiang et al., Water Res 47:4331–4339, 2013, http://dx.doi.org/10.1016/j.watres.2013.05.024). However, the details of the antimicrobial mechanisms of FNA are largely unknown. In this study, we identified the key responses (decreased anaerobic respiration, reducing FNA, combating oxidative stress, and shutting down protein synthesis) of *Desulfovibrio vulgaris* Hildenborough, a model sewer corrosion bacterium, to FNA exposure by examining the growth, physiological, and gene expression changes. These findings provide new insight and underpinning knowledge for understanding the responses of *D. vulgaris* to FNA exposure, thereby benefiting the practical application of FNA for improved control of sewer corrosion and odor.

Sulfate-reducing bacteria (SRB) are anaerobic chemoorganotrophic microorganisms that typically use sulfate as the terminal electron acceptor for respiration and generate energy with the production of hydrogen sulfide (2). In confined spaces, the production of hydrogen sulfide can cause odor and corrosion problems. This is particularly the case in sewers and inlet structures of wastewater treatment plants, where the oxidation of sulfide produces sulfuric acid, which corrodes the concrete surfaces of the sewer. This results in serious deterioration of sewer assets that requires very costly and demanding rehabilitation efforts (3, 4). Consequently, there is great interest in the efficient control of SRB and thereby minimizing hydrogen sulfide production in sewers.

Various chemical dosing methods are used to lower hydrogen sulfide production in sewers, and four strategies currently used include sulfide oxidation by the injection of chemical oxidants, such as air, oxygen, or nitrate (5, 6); sulfide precipitation by addition of iron salts (7); application of magnesium hydroxide or lime to raise the wastewater pH and prevent the release of hydrogen sulfide (8); and inhibition of the activities of SRB to lessen the generation of hydrogen sulfide (9). However, to obtain the required sulfide control, these strategies require continuous chemical consumption and considerable operational costs (10).

Free nitrous acid (FNA), the protonated form of nitrite, was recently demonstrated to be the true metabolic inhibitor behind the usually observed nitrite inhibition (11). In recent treatment of sewer biofilms, it was seen that application of FNA for 6 to 24 h at 0.2 to 0.3 mg N/liter decreased the live cell percentage from about 80% to 5 to 15% (3). Since then, FNA has been applied in sewer field trials in which an 80% reduction in sulfide production was achieved by intermittent FNA dosing at 0.26 mg N/liter for 8 to 24 h every 4 weeks (1). These investigations support that the application of FNA for the control of sulfide levels in sewers is highly feasible.

Received 1 June 2016 **Accepted** 28 June 2016

Accepted manuscript posted online 1 July 2016

Citation Gao S-H, Ho JY, Fan L, Richardson DJ, Yuan Z, Bond PL. 2016. Antimicrobial effects of free nitrous acid on *Desulfovibrio vulgaris*: implications for sulfide-induced corrosion of concrete. Appl Environ Microbiol 82:5563–5575. doi:10.1128/AEM.01655-16.

Editor: H. L. Drake, University of Bayreuth

Address correspondence to Philip L. Bond, phil.bond@awmc.uq.edu.au.

Therefore, FNA is emerging as an extremely promising antimicrobial agent for the control of SRB, their activities, and sulfide production, and there is great interest in understanding how SRB respond to and withstand exposure to FNA. Nitrite is reported to cause decreased expression of the genes coding for dissimilatory sulfite reductase (DsrAB genes) and thereby disrupt the respiratory activities of SRB (12, 13). Currently, the antimicrobial effects of FNA on bacteria in general are believed to be multitargeted (14). It is thought that FNA, and perhaps reactive nitrogen species (RNS) derived from FNA, causes oxidative stress, resulting in damage to cell enzymes, cellular membranes and walls, and nucleic acids (15). Other hypotheses to explain the antimicrobial effects include FNA causing disruption of the proton motive force (16), nitrosylation of metal centers or thiol groups in enzymes (17), and DNA mutation (14). However, these hypotheses are not well verified, and it is not clear whether some of these effects are more important than others in different bacteria. Additionally, different bacteria will have different levels of tolerance to FNA (18).

Desulfovibrio species can be prevalent SRB in sewers (19) and are likely important for hydrogen sulfide production in sewage. *Desulfovibrio vulgaris* Hildenborough is well studied and is demonstrated to have a periplasmic cytochrome *c* nitrite reductase (NrfA) for the conversion of nitrite to ammonium (2). It is largely thought that this nitrite reductase activity is not respiratory or for growth (20) but is a mechanism to remove the toxic nitrite (13). However, in a recent twist, there is suggestion that the nitrite reduction activity can conserve energy for growth (21).

To date, there have been some transcriptional investigations, based on macroarray and microarray analyses, to examine the effects of nitrite on *D. vulgaris* (12, 13). These studies indicate that nitrite stress could inhibit sulfate reduction and cause possible oxidative stress, as well as disrupt iron homeostasis. However, all the conclusions and hypotheses drawn from those investigations are based only on the transcriptional responses. A comprehensive and systematic understanding of the antimicrobial mechanisms of FNA on *D. vulgaris* is still lacking. This could be achieved by combining the transcriptional response with the detection of cell activities and physiological changes.

In this study, substrate transformations and physiological changes were detected in response to different levels of FNA. In addition, whole-genome mRNA sequencing (RNA-seq) analysis was also conducted on *D. vulgaris* cultures in the presence and absence of a subbactericidal level of FNA (4.0 μg N/liter). The global transcriptome response was combined with analyses of substrate transformations and physiological responses to test the hypotheses mentioned above. From this, a more comprehensive understanding of the effects of FNA was obtained to verify the key determinants of FNA stress in this model sewer hydrogen sulfide-producing bacterium.

MATERIALS AND METHODS

Cultivation of *D. vulgaris* Hildenborough. *D. vulgaris* Hildenborough (ATCC 29579) was provided by Jizhong Zhou and Aifen Zhou from the Institute for Environmental Genomics, University of Oklahoma. For all experiments, a defined lactate sulfate medium (LS4D medium) (22) was used to cultivate the bacterium. The LS4D medium was prepared, added to serum bottles, and gassed with nitrogen gas for 30 min before capping with butyl rubber stoppers for autoclaving. One-and-a-half milliliters of a glycerol-preserved stock of *D. vulgaris* was used to inoculate the serum bottles containing 140 ml of medium. These were then cultivated at 37°C for 48 h to achieve the early stationary phase of growth (optical density at 600 nm [OD_{600}], 0.9 to 1.0). The OD_{600} of the culture was then adjusted to 0.5, and multiple 10-ml aliquots of this were used to inoculate serum bottles containing 140 ml of fresh LS4D medium. The inoculated bottles were then incubated at 30°C without shaking for further use in the experiments described below. All experimental procedures of culture growth, physiological assays, and RNA-seq analyses were performed on triplicate cultures, unless otherwise mentioned.

FNA treatment on cultures of *D. vulgaris*. After 26 h growth at 30°C, when the cultures were in early log phase (OD_{600}, around 0.3), nitrite was added to achieve starting FNA concentrations of 0, 1.0, 4.0, and 8.0 μg N/liter. The term "starting concentration" is used to describe the levels of FNA added in the different experiments, as during the incubations, the actual FNA concentrations change, most likely due to the nitrite reduction activity of *D. vulgaris*. For each FNA concentration, the culture incubations were performed in triplicate. The FNA concentration is dependent on the level of nitrite, pH, and temperature, and this was calculated based on the equation already described (23). These concentrations of FNA were chosen based on preliminary studies (not shown), where it was observed that these levels of exposure covered the spectrum of growth responses to FNA, from slight inhibition of growth to near-complete killing of the organism. Following the addition of FNA, the cultures were incubated for a further 48 h at 30°C. During exposure to the different FNA levels, the concentrations of lactate, acetate, sulfate, sulfite, sulfide, thiosulfate, nitrite, and FNA were determined from filtered samples of the inoculated cultures. Additionally, samples from the triplicate controls (no added FNA) and FNA-treated cultures (4.0 μg N/liter) were taken for RNA extraction at 1 h after FNA addition. These conditions were chosen for study of the transcriptional response, as (i) it has been previously observed in *D. vulgaris* that the peak of the gene expression response to nitrite occurs at 1 h after nitrite exposure (13), and (ii) our preliminary studies showed that at 4.0 μg N/liter of FNA exposure, there was a significant effect on the organism's growth, but complete killing did not occur, and eventually the organism could overcome the stress. In preparation for the RNA extraction, 5 ml of the bacterial suspension from each serum bottle was centrifuged at 13,000 × *g* for 2 min, the supernatant was discarded, and the pellets were immediately frozen in liquid nitrogen before storage at −80°C. Total RNA extraction was performed from the pellets using the Qiagen miRNeasy minikit (catalog no. 217004), according to the manufacturer's instructions, except for the addition of an extra bead-beating step to ensure the complete lysis of the cells. Strand-specific cDNA libraries were constructed, and Illumina paired-end sequencing (HiSeq 2000; Illumina, Inc., San Diego, CA, USA) was performed (Macrogen, Seoul, South Korea) on the extracted RNA.

Chemical analyses of culture samples. Culture OD_{600} and pH were monitored during the incubations with a Cary 50 Bio UV-visible spectrophotometer (Varian, Australia) and a labCHEM-pH benchtop pH-mV temperature meter, respectively. Slight increases in pH occurred during incubation, which ranged from 7.15 to 7.4 due to the conversion of nitrite to ammonium. For nitrite detection, culture samples were taken, immediately filtered through 0.22-μm-pore-size filters (Merck Millipore, USA), and analyzed on a Lachat QuikChem 8000 flow injection analyzer (FIA). The concentrations of sulfur species (sulfide, sulfite, thiosulfate, and sulfate) were determined in culture samples by ion chromatography. For this, 1.5-ml samples were filtered (0.22-μm-pore size; Merck Millipore) into 2-ml vials that contained 0.5 ml of an antioxidant preservative buffer (24). Samples were then analyzed within 24 h by ion chromatography (Dionex ICS-2000). The culture lactate and acetate levels were determined in 1.0-ml filtered (0.22-μm-pore size; Merck Millipore) samples by high-performance liquid chromatography, as previously described (25).

Physiological assay of *D. vulgaris*. Various assays were conducted during growth of *D. vulgaris* in the absence and presence of different FNA concentrations. LIVE/DEAD staining was conducted on the culture samples, as described in the manufacturer's instructions (BacLight bacterial viability kit, catalog no. L7012; Molecular Probes). The LIVE/DEAD ratio

of cells was then quantified by applying 500 μl of the stained samples to a FACSAria II flow cytometer (BD Biosciences, San Jose, CA, USA). The cellular redox status of the cultures was determined by staining 500 μl of samples with the RedoxSensor green reagent provided in the BacLight RedoxSensor green vitality kit (catalog no. B34954; Life Technologies), as per the manufacturer's instructions. The fluorescence signal of the stained cultures was quantified using the FACSAria II type flow cytometer, as suggested in the kit protocol. Cellular ATP levels were determined in 500 μl of culture samples using the BacTiter-Glo microbial cell viability assay (catalog no. G8231; Promega Corporation). Cellular thiol group levels were determined on 200-μl culture samples using the thiol and sulfide quantitation kit (catalog no. T-6060; Molecular Probes). The ATP and thiol group assays were performed as described in the corresponding manufacturers' instructions.

RNA-seq data processing and differentially expressed gene analysis. The raw sequence reads were treated using the NGS QC toolkit (version 2.3.3) (26) to trim the 3′-end residual adaptors and primers and remove the ambiguous characters in the reads. Then, the sequence reads consisting of at least 85% bases with a quality value of ≥20 were kept. The resulting clean reads no shorter than 75 bp were used for downstream analyses. SeqAlto (version 0.5) was used to align the clean reads of each sample to the reference genome (NC_002937) of *D. vulgaris* (27). Cufflinks (version 2.2.1) was used to calculate the strand-specific coverage for each gene and to analyze the differential expression on triplicate cultures (28). The CummeRbund package in R (http://compbio.mit.edu/cummeRbund/) was used to conduct the statistical analyses and visualization. Gene expression was calculated as reads per kilobase of a gene per million mapped reads (RPKM), a normalized value generated from the frequency of detection and the length of a given gene (28). Differences in fold change values were calculated between control and FNA-treated samples (4.0 μg N/liter) by determining the $\log_2$ fold change (LFC) of the averaged RPKM values of two triplicate experiments. A stringency LFC cutoff of ≥1 or less than or equal to −1, with *q* value less than 0.05, was used to identify the significantly differentially expressed genes.

Accession number(s). The raw sequencing data were deposited in NCBI's Gene Expression Omnibus (GEO) and are accessible through GEO series accession no. GSE78834.

RESULTS

Concentration-dependent effects of FNA on culture growth and respiratory activities. In these investigations, *D. vulgaris* utilizes sulfate as the electron acceptor and lactate as the electron donor, with sulfide and acetate as the respective end products (2). Additionally, *D. vulgaris* has NrfA that can reduce nitrite to ammonium, allowing it to survive in environments in the presence of nitrite (2). The growth of *D. vulgaris* cultures exposed to the lowest starting FNA concentration of 1.0 μg N/liter was slightly inhibited during the 48 h of incubation (Fig. 1). Inhibition of growth increased with the increasing levels of FNA, and growth was almost completely stopped with FNA at 8.0 μg N/liter (Fig. 1).

In the presence of FNA at 1.0 μg N/liter, the levels of lactate oxidation and sulfate reduction were slightly less than those of the control culture (no FNA addition) (Fig. 2C and E), and this coincided with the observed slight decreased growth (Fig. 1), indicating that FNA was having only a slight inhibitory effect on the organism at this level. During the incubation, 1.0 μg N/liter FNA was completely reduced within 8 h after addition (Fig. 2A and B). In comparison, much lower lactate oxidation levels were detected in cultures with starting FNA concentrations of 4.0 and 8.0 μg N/liter (Fig. 2C). In these cultures, there would be limited electrons available for sulfate reduction, which was severely diminished (Fig. 2E), and this coincided with the reductions in growth levels detected (Fig. 1). In the batch cultures, nitrite reduction

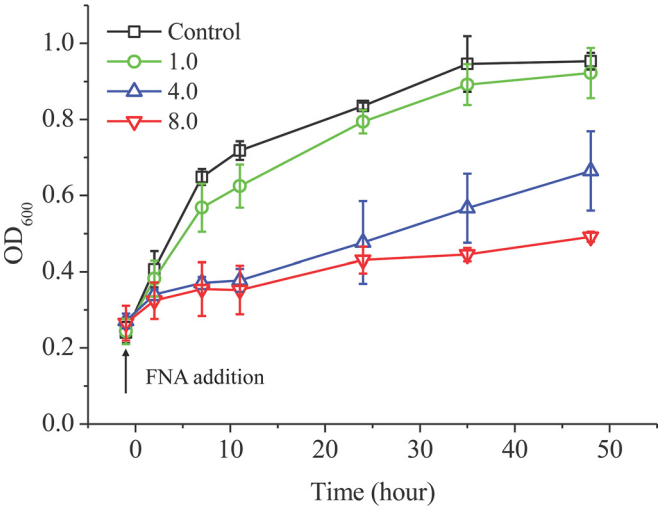

FIG 1 Growth profiles of *D. vulgaris* batch cultures in the presence of different starting FNA concentrations (μg N/liter). FNA was added at time 0 h. The control culture has no FNA addition. Error bars show the standard deviations of the results from triplicate cultures. The key shows the FNA starting concentrations.

occurred (Fig. 2A and B) after FNA addition. This was evident at all FNA concentrations and was likely due to the nitrite reductase activity of *D. vulgaris*.

The absolute ratios of lactate consumed, sulfate used, and acetate produced were calculated from the concentrations detected during the 48-h incubations of *D. vulgaris* at the different FNA levels. The ratios were compared to the theoretical ratio determined when acetate is considered to be the product of the lactate oxidation (Table 1). For the control culture not exposed to FNA, these values are reasonably close to the stoichiometric ratios for lactate oxidation (Table 1). However, the ratios of lactate used and acetate produced were increased at the higher level of applied FNA. This could be explained if there was increased competition for electrons during FNA exposure, which may likely have resulted from increased nitrite reduction activity.

Sulfite and thiosulfate levels were detected during the batch incubations (Fig. 2G and H). There were no obvious differences in the levels of sulfite that correlated with the different FNA levels, while thiosulfate was detected only in the cultures that were exposed to FNA levels of 4 and 8 μg N/liter (Fig. 2H).

Changes in specific cell activities during FNA exposure. LIVE/DEAD staining was performed on the *D. vulgaris* batch cultures to evaluate the effect of FNA on cell viability. At early log phase prior to FNA addition, the viable cell numbers in the cultures were around 85% to 90% (Fig. 3A). When no FNA was added, the live cell percentage stayed at this level until 24 h of incubation before dropping to around 65% at 48 h of incubation (Fig. 3A). This drop in live cells might have resulted from changes in the culture conditions, such as lactate depletion (Fig. 2C). In comparison, the viable cell numbers for the FNA concentration of 1.0 μg N/liter decreased quickly to around 60% when the incubation time was 7 h, and this remained near that level through the incubation period (Fig. 3A). Substantial decreases in the percentage of live cells were detected immediately upon the addition of FNA at 4.0 μg N/liter FNA and at 8.0 μg N/liter, such that near 95% killing of the *D. vulgaris* cultures occurred within 12 h of

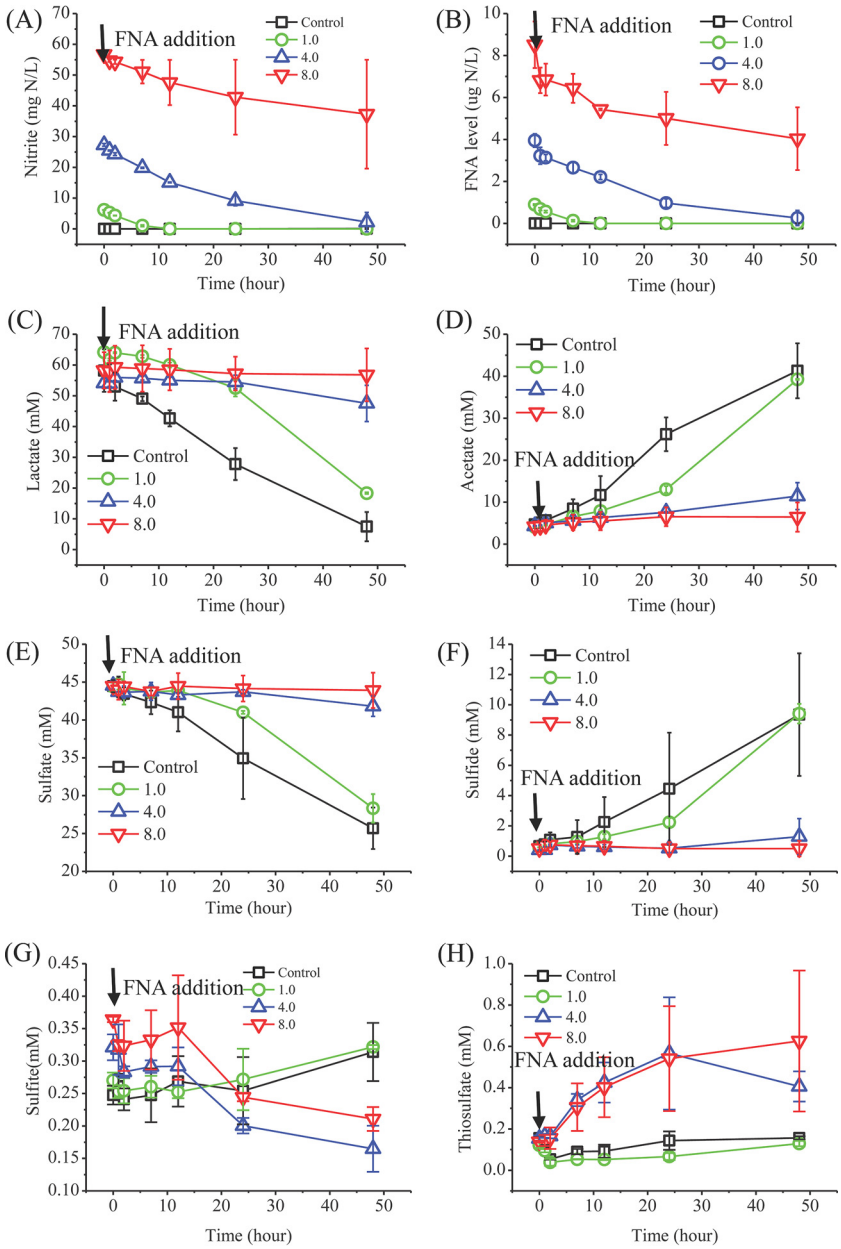

FIG 2 Levels of nitrite (A), FNA (B), lactate (C), acetate (D), sulfate (E), sulfide (F), sulfite (G), and thiosulfate (H) in *D. vulgaris* batch cultures grown on lactate and sulfate. The batch cultures were exposed to different levels of FNA that was added at time 0 h, which was 26 h after inoculation. No FNA was added to the control cultures. Error bars represent the standard deviations of analyses performed from triplicate batch cultures. The keys at the top of the panels show the FNA starting concentrations (micrograms of N/liter).

incubation (Fig. 3A). These results support the suggestion that the bacteriostatic and bactericidal effects of FNA are concentration determined and population specific, as previously detected in *Pseudomonas aeruginosa* PAO1 (23).

Cellular thiol levels of *D. vulgaris* increased with the addition of FNA (Fig. 3B). At FNA starting concentrations of 1.0 and 4.0 μg N/liter, a small increase in cellular thiol levels was detected at 12 and 24 h of incubation (Fig. 3B). However, cellular thiol levels increased markedly throughout the incubation period when the cells were exposed to 8.0 μg N/liter FNA (Fig. 3B). It is thought that FNA could nitrosylate thiol groups, such as those on proteins,

TABLE 1 Absolute ratios of lactate and sulfate used and acetate produced during the 48 h of incubation of *D. vulgaris* cultures in the presence and absence of added FNA

Culture condition	Lactate used (mM)	Sulfate used (mM)	Acetate produced (mM)
Theoretical ratio[a]	2	1	2
Control, no FNA	3.00 ± 1.17	1.00 ± 0.31	2.60 ± 1.21
FNA at 1.0 μg N/liter	2.83 ± 0.13	1.00 ± 0.08	2.19 ± 0.00
FNA at 4.0 μg N/liter	3.00 ± 0.31	1.00 ± 0.27	2.61 ± 0.59
FNA at 8.0 μg N/liter	3.51 ± 1.56	1.00 ± 1.17	3.44 ± 1.49

[a] The theoretical ratio is based on the stoichiometry if acetate is the product.

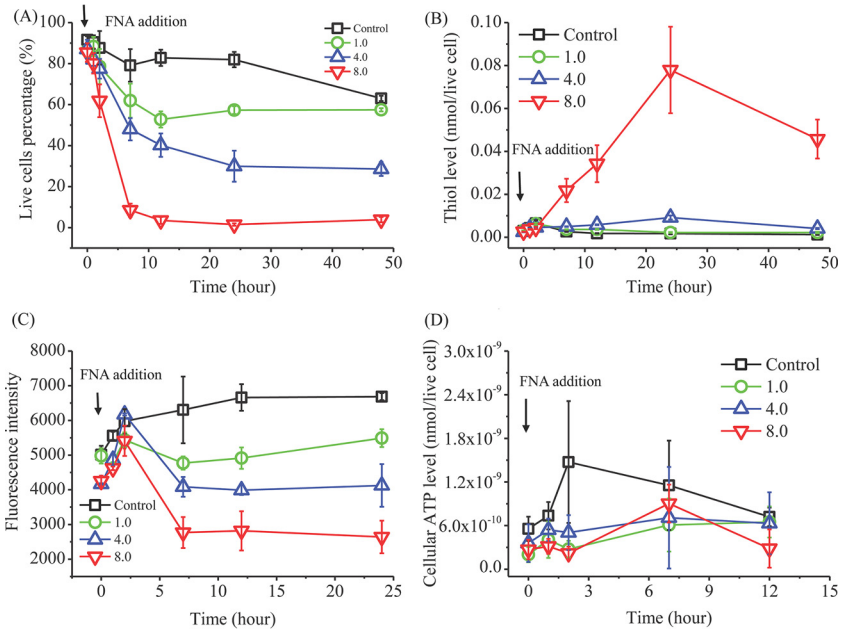

FIG 3 Physiological features of *D. vulgaris* measured during the batch culture incubations in the presence of different starting FNA levels and when no FNA was added (control). The percentage of live cells (A), cellular thiol levels (B), intracellular redox levels, where higher fluorescence indicates lower redox potential (C), and cellular ATP levels (D). FNA was added at time 0 h. Error bars represent the standard deviations of analyses performed from triplicate batch cultures. The keys at the top of the panels show the FNA starting concentrations (micrograms of N/liter).

which might change the activity or function of those (14). There is also a hypothesis that FNA imposes oxidative stress on bacterial cells (29). Thus, in these batch cultures, the cell redox status was determined, and it was observed that with increasing levels of FNA, the cells were more oxidized (Fig. 3C). Cellular ATP levels of the *D. vulgaris* batch cultures (normalized to per live cell) decreased with the increase in added FNA concentrations (Fig. 3D). This supports the idea that FNA acts as a protonophore to decouple the proton motive force across cell membranes and thereby inhibit ATP synthesis (16).

Global transcriptomic analysis of FNA stress. To determine the antimicrobial mechanisms of FNA and the possible response pathways adopted by *D. vulgaris*, gene expression profiles were examined by RNA sequencing. To focus on the direct inhibitory mechanisms of FNA on *D. vulgaris*, we sought to measure changes that report on the primary effect of FNA, not any secondary effects that would occur over longer timescales more related to changes in growth rate, substrate, products, and batch conditions, rather than the direct response to FNA. We therefore measured the transcriptional response after only 1 h of the FNA addition. This was performed when the cultures were exposed to 4.0 μg N/liter at 1 h after FNA addition and compared to gene expression of control cultures when no FNA was added. A total of 239 genes, 6.6% of the total 3,623 genes, were detected as significantly differently expressed (see criteria in Materials and Methods). One hundred fifty-nine genes showed increased transcripts, and 80 genes showed decreased transcript levels in response to FNA stress.

Evidence of oxidative stress and detoxification of FNA by *D. vulgaris*. *D. vulgaris* possesses NrfA that can catalyze the six-electron reduction of nitrite to ammonium, and hydroxylamine is an intermediate of the reduction (30). In these FNA-added cultures, the gene coding for NrfA (DVU0625) exhibited considerable upregulation (Table 2), implying its detoxifying role by the reduction of nitrite (and proportional reduction of FNA). This observation agrees with the decreasing nitrite levels detected in the batch cultures (Fig. 2A). Additionally, the gene, DVU2543, which codes for what is known as the hybrid cluster protein (HCP), was the most upregulated gene detected when exposed to FNA (Table 2). The HCP is proposed to have hydroxylamine reductase activity (31) and was possibly acting to remove hydroxylamine as part of the detoxification of nitrite.

Various genes coding for response to oxidative stress displayed highly increased transcript levels in the FNA-added cultures (e.g., DVU0772 and *ahpC* [DVU2247]; Table 2). This implies that FNA caused oxidizing conditions, which is what was detected by the cellular redox measurement in FNA-added cultures (Fig. 3C). The genes *msrA* (DVU1984) and *msrB* (DVU0576), coding for reductases, which reduce methionine sulfoxides as an antioxidant response, were observed to have increased transcript levels in FNA-added cultures. Additionally, genes of the Fur regulon, DVU0273, *gdp* (DVU0763), and DVU2574, showed increased transcript levels in response to FNA (Table 2), indicating the possibility that FNA causes a response relating to iron levels change in the cell. Alternatively, this might be a response to increased oxidative condition, as the genes involved in oxidative stress and iron homeostasis are of the same superfamily of metalloregulatory proteins (13).

FNA inhibited anaerobic respiration and energy generation. In the presence of FNA, various genes coding for enzymes involved in lactate oxidation and sulfate reduction processes were downregulated (Table 3). This included the genes DVU0849 and DVU0850 and DVU1286 to DVU1290 that code for the quinone-interacting membrane-bound oxidoreductase complex (Qmo) and the sulfite reductase complex (DsrAB), respectively (Table 3).

TABLE 2 The transcriptional responses of *D. vulgaris* genes involved in detoxification when exposed to FNA for 1 h with an initial concentration of 4.0 μg N/liter

Gene ID	Gene name	Annotation	RPKM		LFC	Fold change	*q* value
			Control	FNA added			
Oxidative stress							
DVU2247	*ahpC*	Antioxidant AhpCTSA family protein	643.79	2,376.65	1.88	3.68	0.0003
DVU1397	*bfr*	Bacterioferritin	148.13	381.75	1.37	2.58	0.0003
DVU3183	*sor*	Desulfoferrodoxin	1,237.40	3,966.13	1.68	3.21	0.0003
DVU0772		Hypothetical protein	1,622.19	8,374.84	2.37	5.17	0.0003
DVU0576	*msrB*	Methionine sulfoxide reductase B	15.78	649.09	5.36	41.07	0.0003
DVU1984	*msrA*	Peptide methionine sulfoxide reductase MsrA	24.08	181.96	2.92	7.57	0.0003
DVU1457	*trxB*	Thioredoxin reductase	81.88	415.55	2.34	5.08	0.0003
Fur regulon							
DVU0942	*fur*	Fur family transcriptional regulator	199.36	340.38	0.77	1.71	0.0241
DVU2574		Ferrous ion transport protein	123.57	708.01	2.52	5.74	0.0003
DVU2680	*fld*	Flavodoxin, iron repressed	166.69	1,892.42	3.50	11.31	0.0003
DVU0763	*gdp*	Diguanylate cyclase	21.37	185.5	3.12	8.69	0.0003
DVU0273		Conserved hypothetical protein	37.96	244.7	2.69	6.45	0.0003
Nitrite reduction							
DVU0625		Cytochrome *c* nitrite reductase, catalytic subunit NfrA	94.88	1,874.77	4.30	19.70	0.6357
DVU2543		Hydroxylamine reductase	8.44	8,588.86	9.99	1,016.93	0.0003
DVU2544		Iron-sulfur cluster-binding protein	4.29	1,133.96	8.05	264.58	0.0003

It is proposed that Qmo transfers electrons from lactate oxidation directly to adenosine-5′-phosphosulfate reductase, while DsrAB transfers electrons to the sulfite reductase (2).

Recently, an operon has been described for lactate oxidation genes (*luo*) in *D. vulgaris* (32). This includes the genes DVU3026 for lactate permease, DVU3027, DVU3028, DVU3032, and DVU03033 for lactate dehydrogenase subunits, DVU3025 for pyruvate-ferredoxin oxidoreductase, DVU3030 for acetate kinase, and DVU3029 for phosphate acetyltransferase. Downregulation of all these genes in the *luo* operon, except DVU3026, was observed when exposed to FNA (Table 3). Other genes proposed for lactate oxidation, such as DVU0600 for lactate dehydrogenase and DVU1569 and DVU1570 for pyruvate-ferredoxin oxidoreductase, were upregulated or had no change, respectively, in the presence of FNA. However, DVU0600, DVU1569, and DVU1570 had very low expression values (Table 3), and as discussed later, there is some question regarding the involvement of the proteins coded by these genes in lactate oxidation.

Downregulation of these genes involved in lactate oxidation and transfer of electrons for sulfate reduction correlated with reductions of lactate and sulfate utilization (Fig. 2C and E) and lowered acetate and sulfide production (Fig. 2D and F) when *D. vulgaris* was exposed to FNA. Additionally, the transcripts of genes DVU0774 to DVU0780, and DVU0918, coding for ATP synthase, were all markedly downregulated (Table 3). This coincided with the lowered ATP level detected in the cells. It seems the cells were shutting down the main energy-conserving reactions when exposed to FNA.

FNA disrupts DNA replication, transcription, and translation. Genes encoding critical enzymes involved in DNA replication (e.g., chromosomal replication initiator protein DnaA, DNA polymerase, DNA gyrase, and DNA topoisomerase) and transcription (DNA-directed RNA polymerase) exhibited downregulation after FNA exposure for 1 h (Table 4). As well, the genes coding for 30S and 50S ribosomal structure proteins (Table 4) and a variety of amino acid tRNA synthetases showed significantly decreased transcripts. It is apparent that FNA could be causing decreased cell activities of DNA replication, transcription, and protein biosynthesis in *D. vulgaris*. The phenomenon of decreased DNA replication, transcription, and protein synthesis coincides with the decreased growth and overall metabolism we detected, such as the decreased ability to utilize sulfate and lactate, during FNA exposure (Fig. 1 and 2). The gene *yfi* (DVU1629), coding for the ribosomal subunit interface protein, displayed 14.4-fold upregulation (Table 4). This factor is demonstrated to stabilize ribosomes and stop translation under stressful conditions (33). Possibly, *D. vulgaris* is ceasing translation and inactivates/conserves the existing ribosomes in the presence of FNA. Consequently, we measured protein levels per live cell of the control and FNA-exposed (4.0 μg N/liter) cultures after 2- and 8-h incubation periods (Table 5). The protein levels per cell were less in the FNA-added culture in comparison to the control, suggesting that protein synthesis was markedly arrested when exposed to FNA. This is in agreement with the decreased expression we detected of many genes involved with ribosome function (Table 4).

Additionally, the genes coding for DNA repair proteins MutL (DVU0483) and RadC (DVU1193) showed increased transcript levels when FNA was applied (Table 4). This was also the case for genes coding for chaperone proteins DnaK (DVU0811) and DnaJ (DVU1876) (Table 4) that are reported to assist in the refolding of damaged proteins (34). The upregulation of these genes indicates that FNA is likely causing damage to DNA and proteins and *D. vulgaris* was attempting the repair of these molecules.

DISCUSSION

In this study, the antimicrobial effects of FNA were determined in the model SRB *D. vulgaris*. For the first time, we use a comprehensive approach by combining substrate consumption, physiological analyses, and whole-genome RNA-seq, in the presence and absence of FNA, to discover the antimicrobial mechanisms of

TABLE 3 FNA effects on the transcriptional responses of *D. vulgaris* genes involved in metabolism when exposed to FNA for 1 h with an initial concentration of 4.0 μg N/liter[a]

Gene ID	Gene name	Annotation	RPKM		LFC	Fold change	*q* value
			Control	FNA added			
Sulfate reduction							
DVU0847	*apsA*	Adenylylsulfate reductase subunit alpha	6,909.68	5,078.47	−0.44	−1.36	0.3464
DVU0846	*apsB*	Adenylylsulfate reductase subunit beta	9,741.20	7,860.48	−0.31	−1.24	0.5378
DVU1288	*dsrJ*	Cytochrome *c* family protein (DsrJ)	534.27	61.42	−3.12	−8.70	0.6528
DVU0402	*dsrA*	Dissimilatory sulfite reductase subunit alpha	2,089.97	985.96	−1.08	−2.12	0.0128
DVU0403	*dsrB*	Dissimilatory sulfite reductase subunit beta	2,141.02	1,348.20	−0.67	−1.59	0.1274
DVU0848		Heterodisulfide reductase (Qmo)	926.97	528.78	−0.81	−1.75	0.0488
DVU0849		Heterodisulfide reductase, iron-sulfur-binding subunit (Qmo)	559.5	223.45	−1.32	−2.50	0.0035
DVU0850		Heterodisulfide reductase, transmembrane subunit (Qmo)	705.61	301.39	−1.23	−2.35	0.0042
DVU1290	*dsrM*	Nitrate reductase subunit gamma (DsrM)	812.85	115.61	−2.81	−7.03	0.0003
DVU1289	*dsrK*	Reductase, iron-sulfur-binding subunit (DsrK)	344.44	48.62	−2.82	−7.08	0.0003
DVU1287	*dsrO*	Reductase, iron-sulfur-binding subunit (DsrO)	366.72	53.15	−2.79	−6.90	0.6170
DVU1286	*dsrP*	Reductase, transmembrane subunit (DsrP)	423.76	69.34	−2.61	−6.11	0.0003
DVU1597	*sir*	Sulfite reductase, assimilatory type	216.21	113.30	−0.93	−1.91	0.0051
Lactate oxidation							
DVU3030	*ackA*	Acetate kinase	339.10	83.54	−2.02	−4.06	0.0003
DVU3027	*glcD*	Glycolate oxidase subunit GlcD	274.79	125.67	−1.13	−2.19	0.0035
DVU3031		Hypothetical protein DVU3031	136.07	17.79	−2.93	−7.65	0.6411
DVU3032		Hypothetical protein DVU3032	511.29	42.46	−3.59	−12.04	0.6108
DVU3028		Iron-sulfur cluster-binding protein	281.53	136.67	−1.04	−2.06	0.0037
DVU3033		Iron-sulfur cluster-binding protein	273.18	30.99	−3.14	−8.82	0.0003
DVU0600		L-Lactate dehydrogenase	5.29	25.03	2.24	4.72	0.0003
DVU2110		L-Lactate permease	5.39	5.63	0.06	1.04	0.9109
DVU2285		L-Lactate permease	111.29	27.81	−2.00	−4.00	0.0003
DVU2451		L-Lactate permease	281.30	156.81	−0.84	−1.79	0.0229
DVU2683		L-Lactate permease	118.96	20.57	−2.53	−5.78	0.0003
DVU3026		L-Lactate permease	121.11	77.86	−0.64	−1.56	0.0639
DVU3029	*pta*	Phosphate acetyltransferase	236.08	75.62	−1.64	−3.12	0.0003
DVU1569	*porA*	Pyruvate ferredoxin oxidoreductase subunit alpha	40.03	20.68	−0.95	−1.94	0.7719
DVU1570	*porB*	Pyruvate ferredoxin oxidoreductase subunit beta	42.03	26.86	−0.65	−1.56	0.8398
DVU3025	*poR*	Pyruvate ferredoxin oxidoreductase	821.96	337.59	−1.28	−2.43	0.7256
DVU0577		Formate dehydrogenase formation protein FdhE	22.78	53.38	1.23	2.35	0.0012
DVU0587	*fdnG-1*	Formate dehydrogenase subunit alpha	48.25	203.16	2.07	4.20	0.0003
DVU0588		Formate dehydrogenase subunit beta	77.04	318.11	2.05	4.14	0.0003
ATP synthesis							
DVU0918	*atpB*	ATP synthase F_o subunit A	938.08	160.96	−2.54	−5.83	0.0003
DVU0779	*atpF*	ATP synthase F_o subunit B	1,224.30	266.04	−2.20	−4.60	0.6435
DVU0780		ATP synthase F_o subunit B′	730.80	226.18	−1.69	−3.23	0.0003
DVU0920	*atpI*	ATP synthase I	956.69	313.18	−1.61	−3.05	0.6970
DVU0777	*atpA*	F_oF_1 ATP synthase subunit alpha	1,156.37	198.62	−2.54	−5.82	0.0003
DVU0775	*atpD*	F_oF_1 ATP synthase subunit beta	1,069.12	186.45	−2.52	−5.73	0.0003
DVU0778	*atpH*	F_oF_1 ATP synthase subunit delta	1,589.63	295.74	−2.43	−5.38	0.6396
DVU0774	*atpC*	F_oF_1 ATP synthase subunit epsilon	1,510.29	345.95	−2.13	−4.37	0.0003
DVU0776	*atpG*	F_oF_1 ATP synthase subunit gamma	1,369.15	214.02	−2.68	−6.40	0.0003
Electron transfer							
DVU2524		Cytochrome c_3, putative	2.70	3.15	0.22	1.17	1
DVU0434		*ech* hydrogenase subunit EchA	12.66	3.28	−1.95	−3.86	0.6701
DVU0433		*ech* hydrogenase subunit EchB	11.18	2.20	−2.34	−5.07	0.5587
DVU0432		*ech* hydrogenase subunit EchC	15.72	5.16	−1.61	−3.05	0.0431
DVU0431		*ech* hydrogenase subunit EchD	22.67	6.16	−1.88	−3.68	0.0163
DVU0430		*ech* hydrogenase subunit EchE	13.88	5.16	−1.43	−2.69	0.0066
DVU0429		*ech* hydrogenase subunit EchF	13.21	5.81	−1.19	−2.28	0.1921
DVU2796		Electron transport complex protein RnfA	46.78	33.47	−0.48	−1.40	0.2438
DVU2792		Electron transport complex protein RnfC	45.12	43.07	−0.07	−1.05	0.8732

(Continued on following page)

TABLE 3 (Continued)

Gene ID	Gene name	Annotation	RPKM		LFC	Fold change	*q* value
			Control	FNA added			
DVU2793		Electron transport complex protein RnfD	20.48	18.30	−0.16	−1.12	0.7781
DVU2794		Electron transport complex protein RnfG	32.95	30.79	−0.10	−1.07	0.8453
DVU0535		Hmc operon protein 2	15.05	38.37	1.35	2.55	0.0003
DVU0534		Hmc operon protein 3	12.24	37.62	1.62	3.07	0.0003
DVU0532		Hmc operon protein 5	10.58	32.98	1.64	3.12	0.0003
DVU0531		Hmc operon protein 6	14.61	45.6	1.64	3.12	0.0003
Hydrogenases							
DVU1769	*hydA*	Periplasmic [FeFe]hydrogenase, large subunit	17.53	8.14	−1.11	−2.16	0.009
DVU1770	*hydB*	Periplasmic [FeFe]hydrogenase, small subunit	12.08	8.55	−0.50	−1.41	0.6281
DVU2526	*hynA-2*	Periplasmic [NiFe]hydrogenase, large unit, isozyme 2	3.36	4.67	0.47	1.39	0.3684
DVU2525	*hynB-2*	Periplasmic [NiFe]hydrogenase, small unit, isozyme 2	2.26	3.00	0.41	1.33	1
DVU1918	*hysA*	Periplasmic [NiFeSe]hydrogenase, large subunit	575.74	265.41	−1.12	−2.17	0.0062
DVU1917	*hysB*	Periplasmic [NiFeSe]hydrogenase, small subunit	706.06	236.22	−1.58	−2.99	0.0003

[a] Some genes included in the table were not differentially expressed according to the applied criteria for LFC (see Materials and Methods) but were included here to aid illustration of an FNA-affected pathway or mechanism.

FNA on *D. vulgaris* Hildenborough. Our findings of the transcriptome analysis revealed significant multiple responses and detoxification activities of *D. vulgaris* in response to FNA stress, and the resulting observations and hypotheses were supported by the cell activities and physiological changes detected.

Nitrite consumption and increased transcription of genes coding for the nitrite reductase NrfA demonstrated that detoxification of FNA by NrfA was evident in *D. vulgaris* in the presence of FNA, even when electron supply was low, since lactate oxidation was limited (Fig. 2A and C and Table 2). This is a logical response and is in agreement with previous observations of *D. vulgaris* exposed to nitrite (12, 13). Additionally, the most upregulated gene detected, with a >1,000-fold change in the FNA-added cultures, was DVU2543 (Table 2), which encodes a proposed hydroxylamine reductase (31). High expression of this gene in *D. vulgaris* has been reported previously in response to nitrite exposure (12, 13). The enzyme is thought to be either for the reduction of RNS (the hydroxylamine reductase activity) or for reduction of reactive oxygen species (35). There is a strong possibility here that hydroxylamine or other RNS accumulate during FNA exposure, possibly through incomplete reduction of nitrite by NrfA (30). Characterization of the HCP from *E. coli* shows reduction of hydroxylamine with production of ammonium (31). While the enzyme has not been characterized in *D. vulgaris*, one suggestion is that the HCP is acting similarly or in conjunction with NrfA to detoxify the high levels of nitrite.

Genes coding for electron transfer proteins for sulfate reduction, the Qmo and DsrAB membrane complexes, were significantly downregulated (Table 3). This downregulated gene expression is observed in previous studies of nitrite exposure to *D. vulgaris* (12, 13) and would be an appropriate action in cells that experienced diminished electron flow from lactate oxidation. Interestingly, thiosulfate, the intermediary product of the sulfate reduction by the trithionate-reducing pathway (36), was found to accumulate in FNA-treated samples, while sulfite was not (Fig. 2G and H). Previous studies demonstrate two possible pathways of sulfite reduction to sulfide in *D. vulgaris*; one is by direct reduction without intermediates, and the other is via the trithionate pathway, with thiosulfate and sulfite as the intermediates (37). The observed accumulation of thiosulfate supports the inhibitory effect of nitrite on DsrAB and suggests that the trithionate-reducing pathway is the mechanism of sulfite reduction in *D. vulgaris* under these conditions. In summary, the FNA exposure caused the downregulation of these genes, which severely inhibited the lactate oxidation and sulfate reduction processes.

From early annotations of the *D. vulgaris* genome, the genes associated with lactate oxidation have included DVU0600 for lactate dehydrogenase and DVU1569 and DVU1570 for pyruvate-ferredoxin oxidoreductase. In a previous microarray study exposing *D. vulgaris* to nitrite levels (2.5 mM) similar to those used here (2.3 mM), they reported upregulation of these genes (13). We also report upregulation for the gene DVU0600 but no change for the genes DVU1569 and DVU01570. However, the expression levels (RPKM values) of these genes in the presence of FNA were extremely low (Table 3); thus, this questions the involvement of the respective coded proteins in lactate oxidation. Recently, genes of the *luo* operon are deemed to be responsible for lactate oxidation in *D. vulgaris* rather than DVU0600, DVU1569, and DVU1570 (32). In this study, we detected downregulation of most genes in the *luo* operon when exposed to FNA (Table 3), and importantly, these genes had high expression values when lactate and sulfate utilization and when acetate and sulfide production were active (Table 3 and Fig. 2C to F). This downregulation of the *luo* operon genes during FNA exposure is logical when the cells' respiratory activities were lowered, as we observed. Additionally, these findings further support the involvement of the recently described *luo* operon in lactate oxidation (32).

In addition to the downregulation of genes involved in respiration, there is a suggestion that FNA directly affected enzymes involved in lactate oxidation. The lack of sulfate utilization during high levels of FNA exposure can be readily explained by the inhibition of the sulfite reductase activity of DsrAB by nitrite/FNA (12). However, there is the question as to why the lactate oxidation stops during exposure to FNA. Nitrite reductase activity in the

TABLE 4 FNA effects on the transcriptional responses of *D. vulgaris* genes involved in DNA replication, transcription, and translation when exposed to FNA for 1 h with an initial concentration of 4.0 μg N/liter

Gene ID	Gene name	Annotation	RPKM		LFC	Fold change	*q* value
			Control	FNA added			
DVU1469	*rpsA*	30S ribosomal protein S1	66.08	31.43	−1.07	−2.10	0.0012
DVU1302	*rpsJ*	30S ribosomal protein S10	2,247.95	749.15	−1.59	−3.00	0.0003
DVU1327	*rpsK*	30S ribosomal protein S11	1,785.05	802.95	−1.15	−2.22	0.0022
DVU1298	*rpsL*	30S ribosomal protein S12	1,605.02	539.75	−1.57	−2.97	0.0003
DVU1326	*rpsM*	30S ribosomal protein S13	1,579.22	661.60	−1.26	−2.39	0.0008
DVU1316	*rpsN*	30S ribosomal protein S14	2,500.39	558.05	−2.16	−4.48	0.0003
DVU0839	*rpsP*	30S ribosomal protein S16	1,897.36	902.76	−1.07	−2.10	0.0024
DVU0874	*rpsB*	30S ribosomal protein S2	568.75	187.39	−1.60	−3.04	0.0003
DVU1896	*rpsT*	30S ribosomal protein S20	1,074.90	347.59	−1.63	−3.09	0.0003
DVU1309	*rpsC*	30S ribosomal protein S3	1,612.99	373.63	−2.11	−4.32	0.0003
DVU1328	*rpsD*	30S ribosomal protein S4	1,832.03	702.74	−1.38	−2.61	0.0010
DVU1320	*rpsE*	30S ribosomal protein S5	1,254.60	345.84	−1.86	−3.63	0.0003
DVU0956	*rpsF*	30S ribosomal protein S6	846.18	368.63	−1.20	−2.30	0.0003
DVU1299	*rpsG*	30S ribosomal protein S7	1,661.83	516.48	−1.69	−3.22	0.0003
DVU1317	*rpsH*	30S ribosomal protein S8	1,628.86	350.60	−2.22	−4.65	0.0003
DVU2925	*rplA*	50S ribosomal protein L1	1,207.01	322.34	−1.90	−3.74	0.0003
DVU2926	*rplJ*	50S ribosomal protein L10	2,811.97	704.14	−2.00	−3.99	0.0003
DVU2924	*rplK*	50S ribosomal protein L11	2,152.09	479.63	−2.17	−4.49	0.0003
DVU2518	*rplM*	50S ribosomal protein L13	2,740.46	1,358.38	−1.01	−2.02	0.0135
DVU1313	*rplN*	50S ribosomal protein L14	2,360.35	587.04	−2.01	−4.02	0.0003
DVU1310	*rplP*	50S ribosomal protein L16	2,220.49	487.73	−2.19	−4.55	0.0003
DVU1319	*rplR*	50S ribosomal protein L18	1,455.69	380.51	−1.94	−3.83	0.0003
DVU0835	*rplS*	50S ribosomal protein L19	2,049.36	953.53	−1.10	−2.15	0.0037
DVU1306	*rplB*	50S ribosomal protein L2	1,281.60	385.53	−1.73	−3.32	0.0003
DVU2535	*rplT*	50S ribosomal protein L20	1,552.62	508.75	−1.61	−3.05	0.0003
DVU0927	*rplU*	50S ribosomal protein L21	1,418.19	648.20	−1.13	−2.19	0.0020
DVU1308	*rplV*	50S ribosomal protein L22	2,353.89	499.49	−2.24	−4.71	0.0003
DVU1574	*rplY*	50S ribosomal protein L25	2,580.36	657.59	−1.97	−3.92	0.0003
DVU0928	*rpmA*	50S ribosomal protein L27	2,170.58	787.25	−1.46	−2.76	0.0003
DVU1303	*rplC*	50S ribosomal protein L3	2,546.31	731.53	−1.80	−3.48	0.0003
DVU1315	*rplE*	50S ribosomal protein L5	3,189.91	604.46	−2.40	−5.28	0.0003
DVU1318	*rplF*	50S ribosomal protein L6	2,154.53	518.55	−2.05	−4.15	0.0003
DVU2927	*rplL*	50S ribosomal protein L7/L12	4,245.40	1,100.25	−1.95	−3.86	0.0003
DVU1089	*alaS*	Alanyl-tRNA synthetase	69.54	16.30	−2.09	−4.27	0.0003
DVU3166		Alanyl-tRNA synthetase	18.77	2.35	−2.99	−7.97	0.0096
DVU1248	*argS*	Arginyl-tRNA synthetase	108.21	39.12	−1.47	−2.77	0.0003
DVU3367	*aspS*	Aspartyl-tRNA synthetase	87.97	24.05	−1.87	−3.66	0.0003
DVU0808	*gatA*	Aspartyl/glutamyl-tRNA amidotransferase subunit A	31.75	6.67	−2.25	−4.76	0.0003
DVU1885	*gatB*	Aspartyl/glutamyl-tRNA amidotransferase subunit B	72.54	27.09	−1.42	−2.68	0.0003
DVU0001	*dnaA-1*	Chromosomal replication initiator protein DnaA	42.34	14.96	−1.50	−2.83	0.0003
DVU2252	*dnaA-2*	Chromosomal replication initiator protein DnaA	108.04	45.84	−1.24	−2.36	0.0005
DVU0004	*gyrA*	DNA gyrase subunit A	71.66	10.01	−2.84	−7.16	0.0003
DVU0003	*gyrB*	DNA gyrase subunit B	76.62	12.47	−2.62	−6.14	0.0003
DVU0483	*mutL*	DNA mismatch repair protein MutL	10.08	34.23	1.76	3.40	0.0003
DVU0002	*dnaN*	DNA polymerase III subunit beta	190.12	35.75	−2.41	−5.32	0.0003
DVU1193	*radC*	DNA repair protein RadC	38.21	109.95	1.52	2.88	0.0003
DVU1899		DNA repair protein RecO	17.57	3.75	−2.23	−4.68	0.0090
DVU3389	*topA*	DNA topoisomerase I	81.00	25.61	−1.66	−3.16	0.0003
DVU2316	*topB*	DNA topoisomerase III	11.52	5.40	−1.09	−2.13	0.0037
DVU1730		DNA-binding protein	18.40	122.18	2.73	6.64	0.0003
DVU3193		DNA-binding protein	11.67	31.95	1.45	2.74	0.0003
DVU0396	*hup-1*	DNA-binding protein HU	665.69	1,768.32	1.41	2.66	0.0008
DVU0764	*hup-2*	DNA-binding protein HU	985.51	449.55	−1.13	−2.19	0.0010
DVU0749		DNA-binding response regulator	4.76	17.72	1.90	3.73	0.0003
DVU0596	*lytR*	DNA-binding response regulator LytR	26.69	82.99	1.64	3.11	0.0003
DVU2928	*rpoB*	DNA-directed RNA polymerase subunit beta	253.21	86.11	−1.56	−2.94	0.0003
DVU2929	*rpoC*	DNA-directed RNA polymerase subunit beta′	246.76	74.92	−1.72	−3.29	0.0003
DVU1876	*dnaJ*	DnaJ protein	10.84	123.72	3.51	11.41	0.0003
DVU2150	*dnaK*	DnaK suppressor protein	429.45	203.48	−1.08	−2.11	0.0012

(Continued on following page)

TABLE 4 (Continued)

Gene ID	Gene name	Annotation	RPKM		LFC	Fold change	*q* value
			Control	FNA added			
DVU3256	*mutM*	Formamidopyrimidine-DNA glycosylase	8.23	1.51	−2.45	−5.45	0.0208
DVU2552	*gltX*	Glutamyl-tRNA synthetase	52.07	24.23	−1.10	−2.15	0.0018
DVU0809	*gatC*	Glutamyl-tRNA(Gln) amidotransferase subunit C	56.08	25.83	−1.12	−2.17	0.0381
DVU1898	*glyQ*	Glycyl-tRNA synthetase subunit alpha	124.89	42.47	−1.56	−2.94	0.0003
DVU1897	*glyS*	Glycyl-tRNA synthetase subunit beta	56.85	16.48	−1.79	−3.45	0.0003
DVU1927	*ileS*	Isoleucyl-tRNA synthetase	108.88	40.69	−1.42	−2.68	0.0003
DVU2376	*lysS*	Lysyl-tRNA synthetase	194.54	65.27	−1.58	−2.98	0.0003
DVU0811	*dnaK*	Molecular chaperone DnaK	205.16	1,065.21	2.38	5.19	0.0003
DVU1608	*ligA*	NAD-dependent DNA ligase	21.23	4.26	−2.32	−4.99	0.0003
DVU1573	*pth*	Peptidyl-tRNA hydrolase	152.40	46.24	−1.72	−3.30	0.0003
DVU2534	*pheS*	Phenylalanyl-tRNA synthetase subunit alpha	145.09	29.67	−2.29	−4.89	0.0003
DVU2533	*pheT*	Phenylalanyl-tRNA synthetase subunit beta	68.78	13.54	−2.34	−5.08	0.0003
DVU2904		rRNA large subunit methyltransferase N	21.51	7.33	−1.55	−2.93	0.0008
DVU1629	*yfiA*	Ribosomal subunit interface protein	564.32	8,136.85	3.85	14.42	0.0003
DVU0897		RNA modification protein	10.62	3.19	−1.74	−3.33	0.0072
DVU1257		RNA-binding protein	1,913.15	793.62	−1.27	−2.41	0.0003
DVU2246		S1 RNA-binding domain-containing protein	7.47	2.84	−1.39	−2.63	0.0058
DVU0904	*recJ*	Single-stranded-DNA-specific exonuclease RecJ	13.58	5.17	−1.39	−2.63	0.0024
DVU2538	*thrS*	Threonyl-tRNA synthetase	340.59	138.11	−1.30	−2.47	0.0012
DVU0807	*trmU*	tRNA (5-methylaminomethyl-2-thiouridylate)-methyltransferase	29.96	2.81	−3.41	−10.64	0.0003
DVU1079	*trmE*	tRNA modification GTPase TrmE	7.35	2.51	−1.55	−2.93	0.0196
DVU1828	*gidA*	tRNA uridine 5-carboxymethylaminomethyl modification protein GidA	56.17	17.69	−1.67	−3.18	0.0003
DVU0142	*trpS*	Tryptophanyl-tRNA synthetase	137.87	41.34	−1.74	−3.33	0.0003
DVU2842		Type II DNA modification methyltransferase	119.70	57.17	−1.07	−2.09	0.0018
DVU0953	*tyrS*	Tyrosyl-tRNA synthetase	207.39	57.07	−1.86	−3.63	0.0003
DVU0732	*valS*	Valyl-tRNA synthetase	76.91	30.16	−1.35	−2.55	0.0003

periplasm would act to consume the protons and electrons produced by lactate oxidation in the cytoplasm, as described in the model for respiration by *D. vulgaris* (12). Thus, lactate oxidation should continue unless FNA or nitrite was having an effect on the enzymes involved in that process. The periplasmic hydrogenases are involved in the flow of protons and electrons produced by lactate oxidation (12). However, gene expression of the highly expressed periplasmic hydrogenase, detected as the Ni-Fe-Se type (Table 3), was significantly decreased. Additionally, it has been seen that the activity of these hydrogenases of *D. vulgaris* is inhibited by nitrite and other RNS (38). Consequently, this lowered gene expression and the enzyme inhibition might lower the flow of electrons and protons and explain the lowered lactate oxidation activity in the presence of FNA.

To conserve energy, *D. vulgaris* performs incomplete lactate oxidation to produce acetate and uses sulfate as the electron acceptor. In our batch cultures, there is limited utilization of lactate and sulfate and production of acetate and sulfide at 24 h of exposure of 4.0 μg N/liter FNA (Fig. 2). However, based on 4 electrons being released per molecule of lactate utilized, and 6 and 8 electrons required for nitrite and sulfate reductions, respectively, we calculated the electron balance when the culture was exposed to FNA at 4.0 μg N/liter at 48 h of incubation. It was deduced that even this small amount of lactate utilization, 7.12 mmol, would provide 28.5 mmol of electrons, which is essentially nearly enough required for the nitrite and sulfate reduction (32.5 mmol) that was detected.

During FNA exposure, the cellular redox state was markedly more oxidized (Fig. 3C), and genes coding for response to oxidative stress and those involved in protein repair had increased expression (Table 2). Additionally, as elucidated above, another possibility for the highly upregulated gene DVU2543 is that the HCP is acting to relieve oxidative stress (35). Considering these detected events, oxidative stress is suggested to be an important antimicrobial effect caused by FNA in *D. vulgaris*. While it is currently not known, it is possible that oxidative damage to the cell components was caused by RNS (14, 23). Interestingly, when *Pseudomonas aeruginosa* was recently exposed to FNA, a more

TABLE 5 Protein levels measured in control and FNA-treated cells after 2 and 8 h of incubation

Culture type	Protein level (pg/cell)			
	2 h	8 h	Amt of protein change over 6 h of incubation[a]	Protein change expected due to half-life[b]
Control	2.33 ± 0.35	1.97 ± 0.29	−0.36	−0.35
FNA added (4.0 μg N/liter)	2.11 ± 0.18	1.55 ± 0.10	−0.56	−0.32

[a] Protein change detected during the 6 h of incubation.
[b] Protein change predicted (given average protein half-life of 20 h [41]).

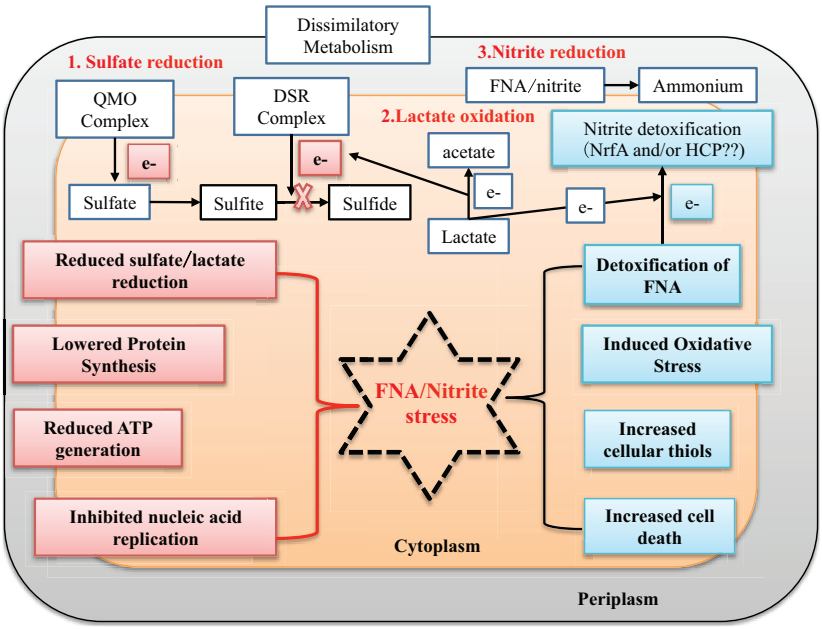

FIG 4 Proposed antimicrobial effects of FNA on *D. vulgaris* based on interpretations of measured physiological activities and the transcriptional responses. The colored boxes indicate activities or events where the associated gene expression was primarily increased (blue) or decreased (pink) in response to FNA exposure.

reduced intracellular condition was caused (25). Therefore, the nature of the oxidative stress caused by FNA is strain dependent rather than a general mode of action.

FNA exposure caused decreased expression of genes involved in protein synthesis in *D. vulgaris*. This is consistent with previous studies of the effect of FNA on *Salmonella enterica* and *P. aeruginosa* (25, 39). Additionally, we detected increased expression of the gene *yfi* (DVU1629) (Table 4), the coded protein of which functions to stabilize ribosomes and stop translation under stressful conditions. Thus, it seems that FNA stress caused *D. vulgaris* to stop protein synthesis and to inactivate and stabilize the existing ribosomes. This was supported by the decreased cellular protein levels we measured during FNA exposure (Table 5). The nature of these FNA-caused changes to the gene regulation detected here needs further investigation; possibly, it was a response to lowered cell energetics. Irrespective, the decreased ribosome activity would have a major impact on the organism's ability to produce its main components for successful cellular activity and operation.

Achieving control of the growth and activity of SRB in sewers is extremely important to mitigate costly concrete corrosion. Growth was detected in the *D. vulgaris* batch cultures at all the concentrations of FNA applied in this study (Fig. 1). However, the growth was low at the high FNA starting concentration of 8.0 μg N/liter, when approximately 5% of cells remained live (Fig. 3A). While only low levels of lactate and sulfate were consumed under this condition, it appears that the remaining live cells were able to grow at the high level of FNA. These results suggest that the bactericidal effects of FNA are determined by concentration, and higher concentrations of FNA need to be applied to kill *D. vulgaris*. We recently proposed that heterogeneity in *Pseudomonas aeruginosa* populations explained differential resistance to FNA (23). It is also possible here that differential resistance to FNA is detected in SRB. The occurrence of resistance would be of concern in the application of FNA in the sewers. Recently, in field trials lasting 6 months, the sulfide production from actual sewer biofilms was reduced by 80% after dosing the sewage with FNA at 0.26 mg N/liter (1). Consequently, good levels of sulfide control were achieved, and increased tolerance to the applied FNA was not observed under the dosing regime. Although the laboratory application of FNA is very different from that in the real sewer situation, through the improved understanding gained in this study, there is likely an opportunity to improve on real FNA applications. For example, combining FNA with treatments that cause increased oxidative stress is seen to achieve more effective biofilm control (40).

In conclusion, several key findings were identified in this study regarding the responses of *D. vulgaris* to FNA stress. A conceptual model was proposed that summarizes the antimicrobial effects of FNA on *D. vulgaris* (Fig. 4). During exposure to FNA, *D. vulgaris* switched from a status of prolific growth to a phase of severely inhibited growth. When exposed to FNA at 4.0 μg N/liter, sulfate reduction and lactate oxidation coupled with ATP generation were suppressed, leading to energy starvation in the FNA-added cultures. The expression of genes coding for lactate oxidation and sulfate reduction was subsequently lowered. In response to energy starvation, *D. vulgaris* stabilized its existing ribosomes and ceased translation of proteins. In addition, FNA caused more oxidative conditions in *D. vulgaris*, and there was transcriptional evidence of attempts to alleviate the oxidative stress. The findings of this study not only provide insight and fundamental understanding of the antimicrobial mechanism of FNA but also can assist in the application of FNA in real sewers for the control of sulfide production and corrosion.

ACKNOWLEDGMENTS

We acknowledge the Australian Research Council for funding support through project DP120102832 (Biofilm Control in Wastewater Systems using Free Nitrous Acid–a Renewable Material from Wastewater), and we

thank the China Scholarship Council for scholarship support for Shu-Hong Gao.

We thank Beatrice Keller, Jianguang Li, University of Queensland, for IC and HPLC analysis and Michael Nefedov, University of Queensland, for assistance with the BD FACSAria II flow cytometer and data analysis.

FUNDING INFORMATION

This work, including the efforts of Shu-Hong Gao, Lu Fan, Zhiguo Yuan, and Philip L. Bond, was funded by Australian Research Council (ARC) (DP120102832). This work, including the efforts of Shu-Hong Gao, was funded by China Scholarship Council.

REFERENCES

1. **Jiang G, Keating A, Corrie S, O'halloran K, Nguyen L, Yuan Z.** 2013. Dosing free nitrous acid for sulfide control in sewers: results of field trials in Australia. Water Res **47:**4331–4339. http://dx.doi.org/10.1016/j.watres.2013.05.024.
2. **Heidelberg JF, Seshadri R, Haveman SA, Hemme CL, Paulsen IT, Kolonay JF, Eisen JA, Ward N, Methe B, Brinkac LM, Daugherty SC, Deboy RT, Dodson RJ, Durkin AS, Madupu R, Nelson WC, Sullivan SA, Fouts D, Haft DH, Selengut J, Peterson JD, Davidsen TM, Zafar N, Zhou L, Radune D, Dimitrov G, Hance M, Tran K, Khouri H, Gill J, Utterback TR, Feldblyum TV, Wall JD, Voordouw G, Fraser CM.** 2004. The genome sequence of the anaerobic, sulfate-reducing bacterium *Desulfovibrio vulgaris* Hildenborough. Nat Biotechnol **22:**554–559. http://dx.doi.org/10.1038/nbt959.
3. **Jiang G, Gutierrez O, Yuan Z.** 2011. The strong biocidal effect of free nitrous acid on anaerobic sewer biofilms. Water Res **45:**3735–3743. http://dx.doi.org/10.1016/j.watres.2011.04.026.
4. **Pikaar I, Sharma KR, Hu S, Gernjak W, Keller J, Yuan Z.** 2014. Water engineering. Reducing sewer corrosion through integrated urban water management. Science **345:**812–814.
5. **Gutierrez O, Mohanakrishnan J, Sharma KR, Meyer RL, Keller J, Yuan Z.** 2008. Evaluation of oxygen injection as a means of controlling sulfide production in a sewer system. Water Res **42:**4549–4561. http://dx.doi.org/10.1016/j.watres.2008.07.042.
6. **Mohanakrishnan J, Gutierrez O, Sharma KR, Guisasola A, Werner U, Meyer RL, Keller J, Yuan Z.** 2009. Impact of nitrate addition on biofilm properties and activities in rising main sewers. Water Res **43:**4225–4237. http://dx.doi.org/10.1016/j.watres.2009.06.021.
7. **Zhang L, Keller J, Yuan Z.** 2009. Inhibition of sulfate-reducing and methanogenic activities of anaerobic sewer biofilms by ferric iron dosing. Water Res **43:**4123–4132. http://dx.doi.org/10.1016/j.watres.2009.06.013.
8. **Gutierrez O, Park D, Sharma KR, Yuan Z.** 2009. Effects of long-term pH elevation on the sulfate-reducing and methanogenic activities of anaerobic sewer biofilms. Water Res **43:**2549–2557. http://dx.doi.org/10.1016/j.watres.2009.03.008.
9. **Zhang L, De Gusseme B, De Schryver P, Mendoza L, Marzorati M, Verstraete W.** 2009. Decreasing sulfide generation in sewage by dosing formaldehyde and its derivatives under anaerobic conditions. Water Sci Technol **59:**1248–1254.
10. **Jiang G, Gutierrez O, Sharma KR, Keller J, Yuan Z.** 2011. Optimization of intermittent, simultaneous dosage of nitrite and hydrochloric acid to control sulfide and methane productions in sewers. Water Res **45:**6163–6172. http://dx.doi.org/10.1016/j.watres.2011.09.009.
11. **Vadivelu VM, Yuan Z, Fux C, Keller J.** 2006. The inhibitory effects of free nitrous acid on the energy generation and growth processes of an enriched *Nitrobacter* culture. Environ Sci Technol **40:**4442–4448. http://dx.doi.org/10.1021/es051694k.
12. **Haveman SA, Greene EA, Stilwell CP, Voordouw JK, Voordouw G.** 2004. Physiological and gene expression analysis of inhibition of *Desulfovibrio vulgaris* Hildenborough by nitrite. J Bacteriol **186:**7944–7950. http://dx.doi.org/10.1128/JB.186.23.7944-7950.2004.
13. **He Q, Huang KH, He Z, Alm EJ, Fields MW, Hazen TC, Arkin AP, Wall JD, Zhou J.** 2006. Energetic consequences of nitrite stress in *Desulfovibrio vulgaris* Hildenborough, inferred from global transcriptional analysis. Appl Environ Microbiol **72:**4370–4381. http://dx.doi.org/10.1128/AEM.02609-05.
14. **Fang FC.** 2004. Antimicrobial reactive oxygen and nitrogen species: concepts and controversies. Nat Rev Microbiol **2:**820–832. http://dx.doi.org/10.1038/nrmicro1004.
15. **Zahrt TC, Deretic V.** 2002. Reactive nitrogen and oxygen intermediates and bacterial defenses: unusual adaptations in *Mycobacterium tuberculosis*. Antioxid Redox Signal **4:**141–159. http://dx.doi.org/10.1089/152308602753625924.
16. **Zhou Y, Oehmen A, Lim M, Vadivelu V, Ng WJ.** 2011. The role of nitrite and free nitrous acid (FNA) in wastewater treatment plants. Water Res **45:**4672–4682. http://dx.doi.org/10.1016/j.watres.2011.06.025.
17. **O'Leary V, Solberg M.** 1976. Effect of sodium nitrite inhibition on intracellular thiol groups and on the activity of certain glycolytic enzymes in *Clostridium perfringens*. Appl Environ Microbiol **31:**208–212.
18. **Wang Q, Ye L, Jiang G, Hu S, Yuan Z.** 2014. Side-stream sludge treatment using free nitrous acid selectively eliminates nitrite oxidizing bacteria and achieves the nitrite pathway. Water Res **55:**245–255. http://dx.doi.org/10.1016/j.watres.2014.02.029.
19. **Sun J, Hu S, Sharma KR, Ni BJ, Yuan Z.** 2014. Stratified microbial structure and activity in sulfide- and methane-producing anaerobic sewer biofilms. Appl Environ Microbiol **80:**7042–7052. http://dx.doi.org/10.1128/AEM.02146-14.
20. **Pereira IA, LeGall J, Xavier AV, Teixeira M.** 2000. Characterization of a heme *c* nitrite reductase from a non-ammonifying microorganism, *Desulfovibrio vulgaris* Hildenborough. Biochim Biophys Acta **1481:**119–130. http://dx.doi.org/10.1016/S0167-4838(00)00111-4.
21. **Korte HL, Saini A, Trotter VV, Butland GP, Arkin AP, Wall JD.** 2015. Independence of nitrate and nitrite inhibition of *Desulfovibrio vulgaris* Hildenborough and use of nitrite as a substrate for growth. Environ Sci Technol **49:**924–931. http://dx.doi.org/10.1021/es504484m.
22. **Zhou AF, He ZL, Redding-Johanson AM, Mukhopadhyay A, Hemme CL, Joachimiak MP, Luo F, Deng Y, Bender KS, He Q, Keasling JD, Stahl DA, Fields MW, Hazen TC, Arkin AP, Wall JD, Zhou JZ.** 2010. Hydrogen peroxide-induced oxidative stress responses in *Desulfovibrio vulgaris* Hildenborough. Environ Microbiol **12:**2645–2657.
23. **Gao S-H, Fan L, Yuan Z, Bond PL.** 2015. The concentration-determined and population-specific antimicrobial effects of free nitrous acid on *Pseudomonas aeruginosa* PAO1. Appl Microbiol Biotechnol **99:**2305–2312. http://dx.doi.org/10.1007/s00253-014-6211-8.
24. **Keller-Lehmann B, Corrie S, Ravn R, Yuan Z, Keller J.** 2006. Preservation and simultaneous analysis of relevant soluble sulfur species in sewage samples. Proceedings of the Second International IWA Conference on Sewer Operation and Maintenance, 26 to 28 October 2006, Vienna, Austria.
25. **Gao S-H, Fan L, Peng L, Guo J, Agulló-Barceló M, Yuan Z, Bond PL.** 2016. Determining multiple responses of *Pseudomonas aeruginosa* PAO1 to an antimicrobial agent, free nitrous acid. Environ Sci Technol **50:**5305–5312. http://dx.doi.org/10.1021/acs.est.6b00288.
26. **Patel RK, Jain M.** 2012. NGS QC toolkit: a toolkit for quality control of next generation sequencing data. PLoS One **7:**e30619. http://dx.doi.org/10.1371/journal.pone.0030619.
27. **Mu JC, Jiang H, Kiani A, Mohiyuddin M, Bani Asadi N, Wong WH.** 2012. Fast and accurate read alignment for resequencing. Bioinformatics **28:**2366–2373. http://dx.doi.org/10.1093/bioinformatics/bts450.
28. **Trapnell C, Roberts A, Goff L, Pertea G, Kim D, Kelley DR, Pimentel H, Salzberg SL, Rinn JL, Pachter L.** 2012. Differential gene and transcript expression analysis of RNA-seq experiments with TopHat and Cufflinks. Nat Protoc **7:**562–578. http://dx.doi.org/10.1038/nprot.2012.016.
29. **Poole RK.** 2005. Nitric oxide and nitrosative stress tolerance in bacteria. Biochem Soc Trans **33:**176–180. http://dx.doi.org/10.1042/BST0330176.
30. **Bykov D, Neese F.** 2015. Six-electron reduction of nitrite to ammonia by cytochrome *c* nitrite reductase: insights from density functional theory studies. Inorg Chem **54:**9303–9316. http://dx.doi.org/10.1021/acs.inorgchem.5b01506.
31. **Wolfe MT, Heo J, Garavelli JS, Ludden PW.** 2002. Hydroxylamine reductase activity of the hybrid cluster protein from *Escherichia coli*. J Bacteriol **184:**5898–5902. http://dx.doi.org/10.1128/JB.184.21.5898-5902.2002.
32. **Vita N, Valette O, Brasseur G, Lignon S, Denis Y, Ansaldi M, Dolla A, Pieulle L.** 2015. The primary pathway for lactate oxidation in *Desulfovibrio vulgaris*. Front Microbiol **6:**606.
33. **Agafonov DE, Kolb VA, Spirin AS.** 2001. A novel stress-response protein that binds at the ribosomal subunit interface and arrests translation. Cold Spring Harbor Symp Quant Biol **66:**509–514. http://dx.doi.org/10.1101/sqb.2001.66.509.
34. **Srinivasan SR, Gillies AT, Chang L, Thompson AD, Gestwicki JE.** 2012. Molecular chaperones DnaK and DnaJ share predicted binding sites on

most proteins in the *E. coli* proteome. Mol Biosyst **8:**2323–2333. http://dx.doi.org/10.1039/c2mb25145k.
35. **Aragao D, Mitchell EP, Frazao CF, Carrondo MA, Lindley PF.** 2008. Structural and functional relationships in the hybrid cluster protein family: structure of the anaerobically purified hybrid cluster protein from *Desulfovibrio vulgaris* at 1.35 angstrom resolution. Acta Crystallogr D Biol Crystallogr **64:**665–674. http://dx.doi.org/10.1107/S0907444908009165.
36. **Kim JH, Akagi JM.** 1985. Characterization of a trithionate reductase system from *Desulfovibrio vulgaris*. J Bacteriol **163:**472–475.
37. **Rabus R, Hansen TA, Widdel F.** 2006. Dissimilatory sulfate-and sulfur-reducing prokaryotes, p 659–660. *In* Rabus R, Hansen TA, Widdel F (ed), The prokaryotes. Springer-Verlag, New York, NY.
38. **Tibelius KH, Knowles R.** 1984. Hydrogenase activity in *Azospirillum brasilense* is inhibited by nitrite, nitric oxide, carbon monoxide, and acetylene. J Bacteriol **160:**103–106.
39. **Mühlig A, Behr J, Scherer S, Müller-Herbst S.** 2014. Stress response of *Salmonella enterica* serovar Typhimurium to acidified nitrite. Appl Environ Microbiol **80:**6373–6382. http://dx.doi.org/10.1128/AEM.01696-14.
40. **Jiang G, Yuan Z.** 2013. Synergistic inactivation of anaerobic wastewater biofilm by free nitrous acid and hydrogen peroxide. J Hazard Mater **250–251:**91–98.
41. **Moran MA, Satinsky B, Gifford SM, Luo H, Rivers A, Chan LK, Meng J, Durham BP, Shen C, Varaljay VA, Smith CB, Yager PL, Hopkinson BM.** 2013. Sizing up metatranscriptomics. ISME J **7:**237–243. http://dx.doi.org/10.1038/ismej.2012.94.